

AD-A092 251

MASSACHUSETTS INST OF TECH CAMBRIDGE DEPT OF MATERIA--ETC F/6 11/2  
AN INVESTIGATION OF THE STRUCTURE AND MECHANICAL PROPERTIES OF --ETC(U)  
OCT 80 N J GRANT, J B VANDER, S C ASHDOWN DAAG29-79-C-0077

ARO-16219.1-MS

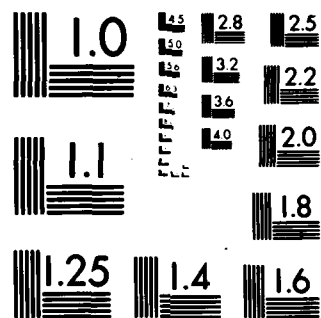
NL

UNCLASSIFIED

For 1  
of 2  
pages



END  
DATE  
FILMED  
1-81  
DTIC



MICROCOPY RESOLUTION TEST CHART

NATIONAL BUREAU OF STANDARDS-1963-A

UNCLASSIFIED

SECURITY CLASSIFICATION OF THIS PAGE (When Data Entered)

ARD 16219.1-MS

10

AD A092251

REPORT DOCUMENTATION PAGE		READ INSTRUCTIONS BEFORE COMPLETING FORM
1. REPORT NUMBER P-16219-MS ✓	2. GOVT ACCESSION NO. AD-A012352 (12)	3. RECIPIENT'S CATALOG NUMBER
4. TITLE (and Subtitle) An Investigation of the Structure and Mechanical Properties of High Temperature Glassy and Micro-crystalline Alloys	5. TYPE OF REPORT & PERIOD COVERED Final Report 5-1-79 to 7-15-80	6. PERFORMING ORG. REPORT NUMBER
7. AUTHOR(s) N. J. Grant, J. B. Vander Sande, C. Ashdown and L. Collins	8. CONTRACT OR GRANT NUMBER(s) DAAG29-79-C-0077 NEW	
9. PERFORMING ORGANIZATION NAME AND ADDRESS N. J. Grant Department of Materials Science and Engineering Massachusetts Institute of Technology (Room 8-305) Cambridge, MA 02139	10. PROGRAM ELEMENT, PROJECT, TASK AREA & WORK UNIT NUMBERS	
11. CONTROLLING OFFICE NAME AND ADDRESS U. S. Army Research Office Post Office Box 12211 Research Triangle Park, NC 27709	12. REPORT DATE October 27, 1980	13. NUMBER OF PAGES
14. MONITORING AGENCY NAME & ADDRESS (if different from Controlling Office) LEVEL	15. SECURITY CLASS. (of this report) Unclassified	15a. DECLASSIFICATION/DOWNGRADING SCHEDULE
16. DISTRIBUTION STATEMENT (of this Report) Approved for public release; distribution unlimited.		
17. DISTRIBUTION STATEMENT (of the abstract entered in Block 20, if different from Report) NA		
18. SUPPLEMENTARY NOTES The view, opinions, and/or findings contained in this report are those of the author(s) and should not be construed as an official Department of the Army position, policy, or decision, unless so designated by other documentation.		
19. KEY WORDS (Continue on reverse side if necessary and identify by block number) <div style="display: flex; justify-content: space-between;"> <div>           glassy alloys            rapid solidification            metallic glass crystallization            Ni<sub>60</sub>Nb<sub>40</sub> </div> <div>           Ni<sub>85</sub>Nb<sub>15</sub>            Fe<sub>80</sub>B<sub>20</sub>            Fe<sub>(1-x)</sub>B<sub>x</sub> </div> <div>           T<sub>g</sub>, T<sub>x</sub>            TEM studies         </div> </div>		
20. ABSTRACT (Continue on reverse side if necessary and identify by block number) This research had two aims: a) development and characterization of high T <sub>g</sub> (or T <sub>x</sub> ) glassy alloys, and, b) identification and development of glassy Fe, Ni and Co base alloys which are capable of undergoing crystallization to a ductile, superfine grain size (less than about 0.1 μm), hot workable alloy product. In the first instance the Ni <sub>60</sub> Nb <sub>40</sub> and Ni <sub>85</sub> Nb <sub>15</sub> composition ranges were studied for glass formation, crystallization and properties. Alloying studies were undertaken to increase T <sub>g</sub> (T <sub>x</sub> ) and to strengthen and stabilize (cont)		

DTIC  
DIRECTORATE  
DEC 1 1980  
C

BDC FILE COPY

DD FORM 1 JAN 73 1473

EDITION OF 1 NOV 65 IS OBSOLETE

UNCLASSIFIED

SECURITY CLASSIFICATION OF THIS PAGE (When Data Entered)

(Abstract Continued)

the glassy state. In the second instance, compositions and glass forming tendencies were studied whereby the lowest possible metalloid content could be achieved while still producing a glass. For example, the classical  $\text{Fe}_{80}\text{B}_{20}$  composition can be kept in the glassy state during melt spinning for compositions as low as 12-14 at. pct. boron.

Accession No.	
NTIC	
DTIC	
Uncl.	
Class.	
Index	
Doc.	
Dist.	
A	

6

An Investigation of the Structure and Mechanical Properties  
of High Temperature Glassy and Microcrystalline Alloys.

9

Final Report. 2 May 79-25 Jul 80.

10

N. J. Grant, J. B. Vander Sande, C. Ashdown ~~and~~ L. Collins

October 27, 1980

11 27 Oct 80

U. S. Army Research Office

15

Contract No. DAAG29-79-C-0077

12 30

Massachusetts Institute of Technology

18 ARO

19 26229.1-MS

APPROVED FOR PUBLIC RELEASE;  
DISTRIBUTION UNLIMITED

109463 alt

TABLE OF CONTENTS

	<u>Page</u>
ABSTRACT.....	1
INTRODUCTION.....	2
EXPERIMENTAL PROCEDURES.....	4
RESULTS.....	6
Ductile Crystalline Alloys.....	6
Crystallization of $\text{Ni}_{60}\text{Nb}_{40}$ .....	7
Mechanical Properties of $\text{Ni}_{60}\text{Nb}_{40}$ .....	9
Alloy Development.....	9
DISCUSSION.....	9
Ductile Crystalline Alloys.....	9
Crystallization of $\text{Ni}_{60}\text{Nb}_{40}$ .....	10
Mechanical Properties.....	11
Alloy Development.....	12
CONCLUSIONS.....	14
REFERENCES.....	15
PERSONNEL.....	16

LIST OF TABLES

- Table 1. Data on experimental Ni-Nb-X alloys.  
Table 2. Crystallization temperatures of Ni-Nb-M alloys.

LIST OF FIGURES

- Figure 1. Typical DSC scan showing three exothermic transformations.  
Figure 2. Normalized resistivity measurements obtained during an isothermal anneal of  $\text{Ni}_{60}\text{Nb}_{40}$  at 895 K.  
Figure 3. Johnson-Mehl-Avrami plot of resistivity data for the first stage of recrystallization in  $\text{Ni}_{60}\text{Nb}_{40}$ .  
Figure 4. Temperature dependence of the time to achieve 50% completion of the first stage of crystallization in  $\text{Ni}_{60}\text{Nb}_{40}$ .  
Figure 5. Effect of annealing at 871 K on the room temperature properties of  $\text{Ni}_{60}\text{Nb}_{40}$  glass.  
Figure 6. Relation of crystallization temperature to melting temperature and atomic volume of alloying elements in Ni-Nb glasses.

An Investigation of the Structure and Mechanical Properties  
of High Temperature Glassy and Microcrystalline Alloys

ABSTRACT

This research had two aims: a) development and characterization of high  $T_g$  (or  $T_x$ ) glassy alloys, and, b) identification and development of glassy Fe, Ni and Co base alloys which are capable of undergoing crystallization to a ductile, superfine grain size (less than about  $0.1 \mu\text{m}$ ), hot workable alloy product. In the first instance the  $\text{Ni}_{60}\text{Nb}_{40}$  and  $\text{Ni}_{85}\text{Nb}_{15}$  composition ranges were studied for glass formations, crystallization and properties. Alloying studies were undertaken to increase  $T_g$  ( $T_x$ ) and to strengthen and stabilize the glassy state. In the second instance, compositions and glass forming tendencies were studied whereby the lowest possible metalloid content could be achieved while still producing a glass. For example, the classical  $\text{Fe}_{80}\text{B}_{20}$  composition can be kept in the glassy state during melt spinning for compositions as low as 12-14 at. pct. boron.



## INTRODUCTION

Recently, considerable attention has been given to the study of metallic glasses. In the 20 years since Duwez first produced an amorphous metallic alloy by rapid quenching of a melt, several techniques have been developed by which substantial quantities of glassy material may be produced facilitating their study in some detail. It has been found that they exhibit a number of attractive properties, including high strength and hardness, good corrosion resistance, and various attractive magnetic properties.

The glassy state is metastable and with sufficient thermal activation will relax to a more stable state. As temperature is increased there is an increasing tendency for the glass to transform to the equilibrium crystalline structure. As crystallization occurs the properties of the glass generally deteriorate and are lost. Even at temperatures sufficiently low so that crystallization does not occur, substantial relaxation is observed in the amorphous structure, and, although the amorphous structure is maintained, there may be significant changes in the properties of the glasses, including a decrease in density [1] and an increase in hardness [2], Young's modulus [3], and the Curie temperature [4]. Severe embrittlement has also been observed to accompany the relaxation in some metal-metalloid glasses annealed at temperatures significantly less than  $T_g$ .

Many of the alloys studied to date have relatively low crystallization temperatures ( $\sim 400$  to  $600$  K) and since relaxation-related property changes may often be observed  $200$  K or more below the crystallization temperature, the application of these alloys is limited to ambient conditions. For this reason it is of value to consider the development of alloys which crystallize at relatively high temperatures. Alternatively, alloys which possess unusual (improved) properties subsequent to crystallization would be of considerable interest; in the crystallized form these would have relatively low volume fractions of brittle intermetallics so as to have appreciable room temperature ductility. The extremely fine-grained structure expected upon crystallization should give very high strength levels (from the Hall-Petch relation). Corrosion and oxidation properties,

due to the fine dispersion of excess phases, would be correspondingly enhanced. The principal goals of this program have been the development and characterization of high temperature metallic glasses and the development of glasses which remain ductile upon crystallization.

The Ni-Nb system is an attractive one for study of the first objective; rapid cooling from the melt will produce glasses over a range of compositions from 40 to 60 at.% Nb which exhibit high crystallization temperatures (900-950 K)[5]. A glass is most readily formed at the eutectic composition  $\text{Ni}_{60}\text{Nb}_{40}$ , and it is this alloy which has been chosen as a basis for study. This part of the program has followed two courses. The first involves the characterization of the properties of the  $\text{Ni}_{60}\text{Nb}_{40}$  glass and the effect of thermal treatments on these properties. Secondly, an attempt was made to further improve the thermal stability of the glass through the addition of selected alloying elements. The simplicity of the basic Ni-Nb glass as compared to other systems which often include 2 or 3 metal elements and 2 or 3 metalloid elements was attractive for such a study as it was felt a study of the effects of adding a third element to the glass might lead to a fundamental understanding of the factors determining stability of the glass structure.

The Ni-Nb system also appeared attractive for the second objective, namely, the development of a glass which transforms to a ductile crystalline structure since the eutectic between the fcc nickel solid solution and  $\text{Ni}_3\text{Nb}$  has been previously investigated [6] under rapid quenching conditions. A metastable hcp phase is formed, which would indicate that the driving force for formation of the equilibrium  $\text{Ni}_3\text{Nb}$  phase is not high, and points to the possibility of glass formation upon ternary alloying. Accordingly, metalloid additions to this eutectic composition ( $\text{Ni}_{85}\text{Nb}_{15}$ ) were attempted, up to the level of the ternary eutectics (see Table 1).

Subsequently, a review of known glass forming systems [7,8] was undertaken, the primary criterion for selection being the lowest volume fraction of intermetallic compounds. The Fe-B system, because of a wide glass-forming composition range [9], was selected. Ternary additions to

further reduce the amount of boron required for amorphous alloy production are being studied.

#### EXPERIMENTAL PROCEDURES

Alloy buttons were initially prepared by arc melting in an argon atmosphere. All glasses studied were produced by a piston and anvil technique or by melt spinning. The melt-spinner in its present configuration has been used for two years and consists of a 25 cm inner diameter OFHC copper band on an aluminum hub. The apparatus is contained in a vacuum system capable of 50 mTorr. Melting is by induction in 1 atm. He (found to give good ribbon quality and secondary cooling [10]). The melt (typically 10 g) is expelled onto the inner surface of the wheel by a He overpressure of 3-10 psi, depending upon crucible orifice and wheel speed. Crucibles are quartz or alumina (for materials incompatible with silica), with either a 1 mm hole or a 6 x 0.5 mm slot. Wheel speeds presently obtainable are 24, 30, 40, and 50 m/sec. The resulting foils were originally detached by a bevel on the wheel, (producing an outward component of velocity), but this produced appreciable curvature in the wider foils. Flat wheels are now used, and the foils are detached by either a teflon or phosphor bronze scraper. For alloys too reactive or refractory to be contained by oxide crucibles, the feasibility of levitation melting [11] and cold crucible [12] techniques has been demonstrated. The former required the use of a capacitor bank to increase levitation coil currents, which proved unreliable. A radio frequency transformer was therefore built.

Amorphous alloys produced to date on the melt-spinner include Pd-Si (effect of ternary additions), Cu-Zr (corrosion behavior) and Ni-Nb, as will be described subsequently. A series of Fe-B alloys, containing 10, 12, 14, and 17 a/o B (the eutectic composition), were melt-spun. As reported by Ray [9], amorphous alloys may be obtained down to (and including) 12 a/o B. This corresponds to 36% second phase content. The 10 a/o B alloy is a metastable solid solution of boron in bcc Fe, again

confirming work by Ray [13]. The level of B for ternary alloying additions has therefore been set at 10 a/o. A series of alloys with 5, 10, 15, and 20 a/o Mo and 10 a/o B has been melt spun.

The crystallization process in  $\text{Ni}_{60}\text{Nb}_{40}$  has been studied using differential scanning calorimetry (DSC), resistivity measurements, and transmission electron microscopy (TEM). Calorimetry was carried out with a Perkin Elmer DSC-2 at heating rates between 1.25 and 80 K/min. Resistivity measurements were used to follow crystallization during isothermal heat treatments using a four point probe system in which Pt wires were spot welded to the sample. The sample was enclosed in a quartz tube with a wire feedthrough at one end, was evacuated and back-filled with argon. The samples were annealed in a tube furnace with resistivity measurements taken at appropriate time intervals.

For isothermal heat treatments strips of ribbon were encapsulated in evacuated Vycor tubing and annealed in a tube furnace. From these strips samples were obtained for subsequent tensile, hardness and embrittlement testing and TEM work.

Samples were thinned for TEM examination by electrolytic jet polishing in either a bath of 10% perchloric acid in methanol or 10% sulphuric acid in methanol cooled to  $-50^{\circ}\text{C}$ . The thinned samples were examined in a Philips EM300. Knoop hardness tests on heat treated material were performed using a 200g load. Tensile tests were performed on 1 mm wide strips using specially made grips on an Instron tensile machine using a strain rate of  $\sim 5 \times 10^{-4}$  in/in/sec. As a means of measuring the effect of annealing on ductility, the annealed samples were bent into a U-shape between two platens which were gradually brought together until the sample fractured. The distance between the plates at fracture (d), was determined. The strain at fracture,  $\epsilon_f$ , may be approximated by

$$\epsilon_f = \frac{t}{d - t}$$

where t is the ribbon thickness.

For studies of the effect of alloying additions, samples were quenched from the melt using a piston and anvil technique. For producing small quantities of a large number of alloys this method is preferred as it is faster, but the properties of the splat tend to be somewhat less uniform than for melt spun ribbons, and regions for study must be carefully selected.

Three series of alloys were prepared: in one series 5% of the nickel in the basic  $\text{Ni}_{60}\text{Nb}_{40}$  was replaced by each element of the transition elements of the third row of the periodic table to give the alloys  $\text{Ni}_{55}\text{Nb}_{40}\text{M}_5$ , where  $\text{M} = \text{Ti, V, Cr, Mn, Fe, Co or Cu}$ ; in a second series in which Nb was replaced by the transition elements of the 3rd, 4th and 5th columns of the periodic table to give the alloys  $\text{Ni}_{60}\text{Nb}_{35}\text{M}_5$ , where  $\text{M} = \text{Ti, Zr, Hf, V, Ta, Cr, Mo, W}$ ; and in a third series which maintained the 60:40 atomic ratio of Ni to Nb but had additions of 2.5, 5 and 10% metalloid elements (Si, Al and B).

The splatted samples were polished to remove surface oxides and X-ray diffraction was used to determine if the alloy was amorphous. The crystallization temperatures of the glassy alloys were determined using the DSC with a scanning rate of 20 K/min.

## RESULTS

### Ductile Crystalline Alloys

As shown in Table 1, attempts to form a ternary glass based on the  $\text{Ni}_{85}\text{Nb}_{15}$  eutectic by the addition of metalloids up to the ternary eutectic were unsuccessful. It is also noteworthy that the addition of 5-10 a/o of metalloids was sufficient to suppress the formation of the metastable hcp phase.

In Fe-B glassy alloys, additions of 10 a/o Mo to an  $\text{Fe}_{90}\text{B}_{10}$  alloy produced partially crystalline ribbons, but additions of 15 and 20 a/o Mo resulted in the metallic state. This appears to be due to a higher liquidus temperature for the latter alloys (i.e., they may not have been totally molten when poured and this series will

be repeated. It should be noted that the Fe10B10Mo composition will contain only 25% second phase.

#### Crystallization of $\text{Ni}_{60}\text{Nb}_{40}$

Differential scanning calorimetry revealed that crystallization occurred in three stages since three distinct peaks were observed as shown on a typical plot in Fig. 1. This suggests that a metastable phase first crystallizes followed by a transformation to the equilibrium phases. At a scanning rate of 20 K/min. the glass transition temperature ( $T_g$ ) was obscured by the onset of crystallization, but at higher scanning rates there is evidence of a  $T_g$ . Due to the temperature limits of the DSC (1000 K), the third step of the crystallization is not complete at the maximum temperature and it is thus not possible to extend a baseline and calculate the heat of reaction. However, using different scanning rates and applying the Kissinger analysis [14] it was possible to estimate an activation energy for the onset of crystallization as 6.50 eV.

Due to instabilities inherent in the use of the DSC at high temperatures it was not possible to follow the crystallization process under isothermal conditions by calorimetry. Resistivity measurements, however, proved effective. Typical resistivity measurements for an isothermal anneal are shown in Fig. 2. The curve shows an initial gradual decrease in resistivity followed by a much sharper drop beginning at  $t = 100$  min. A levelling off of the resistivity is observed at intermediate times followed by another decrease in resistivity as the material is transformed to the equilibrium structure. Further annealing produces no change in resistivity.

An effort was made to correlate the characteristics of the resistivity curve to the results obtained using DSC. Resistivity measurements were made while heating the sample at 1.7 K/min., and the temperatures at which peaks in the DSC scan would be observed were interpolated from scans at 1.25 and 2.5 K/min. It was apparent that the DSC peaks

correspond to the initial sharp drop in resistivity, the intermediate plateau and the second drop, respectively.

Electron microscopy studies have shown no apparent change in the amorphous structure during the initial gradual decrease in resistivity. Samples annealed through the first sharp drop in resistivity to the intermediate plateau revealed the presence of a crystalline phase, but as yet the diffraction pattern has not been identified.

Until further TEM work has been completed it is not possible to fully understand the crystallization process. However, it is possible to gain some understanding of the initial stage of crystallization by examining the isothermal resistivity measurements. A Johnson-Mehl-Avrami analysis which assumes crystallization occurs through a nucleation and growth process may be applied. If such an analysis is valid, the fraction of the material crystallized  $X(t)$  at time  $t$  may be expressed in the relation

$$X(t) = 1 - \exp(-bt^n)$$

where  $b$  is a rate constant and  $n$  an exponent. This equation may be rewritten as

$$\log [-\log (1-X)] = \log \left( \frac{b}{2.303} \right) + n \log(t)$$

and the exponent  $n$  may be evaluated from a plot of  $\log [-\log (1-X)]$  versus  $\log t$ . By assuming that the fraction crystallized was directly related to the drop in resistivity it was possible to obtain such a plot for the first stage of crystallization as shown in Fig. 3. The value of  $n$  was found to vary between 1.0 and 2.0, and in general was close to 1.5.

Activation energy for the crystallization process is obtained from temperature dependence of the time to reach 50% completion of the process using the expression

$$t_{0.5} = A \exp \left( -\frac{E}{kT} \right)$$

From a plot of  $\log t_{0.5}$  against  $1/T$  (Fig. 4) an activation energy of

6.47 eV was obtained, in good agreement with the value obtained from resistivity measurements.

#### Mechanical Properties of $\text{Ni}_{60}\text{Nb}_{40}$

The as-quenched  $\text{Ni}_{60}\text{Nb}_{40}$  metallic glass exhibits both high strength (286,000 psi) and hardness ( $\text{KHN} = 705 \text{ kg/mm}^2$ ) and excellent ductility as measured by the bend test in which the glass could be bent completely back on itself without fracture. However, exposure to high temperature produced substantial changes in these properties.

The effect of annealing at 871 K on the properties of the  $\text{Ni}_{60}\text{Nb}_{40}$  glass is shown in Fig. 5. A plot of resistivity versus time is included. TEM studies have shown crystallization first occurs between times of 120 and 240 mins. Even brief exposure to high temperature produces dramatic changes in the material properties. There is a sharp rise in hardness accompanied by a reduction in ductility and tensile strength. Further annealing produces a reduction in hardness although little change in fracture stress or ductility is observed. Finally, as the first hard intermetallic crystallites precipitate there is an increase in hardness and a further loss of ductility.

#### Alloy Development

The alloys produced to date are summarized in Table 2. Not all of the alloys produced were completely amorphous and these are noted. Also with the exception of the alloys in which Ti, Zr or Hf replaced Nb, no  $T_g$  was apparent in the glasses. For this reason the temperature for the onset of crystallization  $T_x$  and the temperature of the first crystallization peak are given for comparison.

#### DISCUSSION

##### Ductile Crystalline Alloys

Promising ternary (and quaternary) additions to Fe-B are molybdenum [15], zirconium [16], nickel [17], silicon [18], and aluminum [19]. The role



of nickel, in producing an austenitic (fcc) matrix which should not exhibit a ductile to brittle transition [20], is of particular interest. Silicon and aluminum should improve the ease of glass formation, while zirconium and molybdenum form lower volume fractions of intermetallics for a given addition level.

#### Crystallization of $\text{Ni}_{60}\text{Nb}_{40}$

Until detailed TEM studies are completed it is not possible to define the precise micromechanisms by which crystallization occurs. However, at present, sufficient data exist to allow some speculation as to the process involved. It is clear that crystallization involves three exothermic processes. The first of these may be the precipitation of a metastable Ni rich phase.

It has been reported [21] that the initial crystal structure is tetragonal. It seems likely that this phase is Ni-rich since efforts to produce glasses with larger Ni contents than 60 at.% are unsuccessful while glasses have been reported with Nb contents up to 60 at.% [22]. Thus, it would seem that any tendency for phase separation in the glass might produce a highly unstable Ni rich region which crystallizes, surrounded by a more stable Nb-enriched glass. TEM diffraction patterns of samples annealed to the intermediate plateau are complex but it is clear that some glassy material remains. It thus may be concluded that the next step may involve the replacement of the metastable tetragonal phase with the equilibrium  $\text{Ni}_3\text{Nb}$  phase. The final step in the crystallization process is then likely to be the crystallization of the Nb enriched glass to the equilibrium  $\mu\text{-NiNb}$  phase.

The kinetics of the first stage of crystallization have been examined in some detail. The isothermal resistivity measurements show an incubation period prior to the onset of crystallization. This suggests that there are no suitably sized nuclei in the quenched material and a period of time is required for the development of a population of nuclei characteristic of the annealing temperature. It is for this reason that an attempt has

been made to fit the data to the kinetics expected of a nucleation and growth process. The time exponent in the Johnson-Mehl-Avrami expression,  $n = 1.5$ , is considerably lower than that reported for the crystallization of other metallic glasses where the value typically lies between 3 and 4 [23]. A value of  $n = 1.5$  is consistent with diffusion controlled growth of a fixed number of particles [24]. Similar behaviour has been reported in Pd-Ni-P [25] and Pd-Ag-Si [26] glasses. At higher temperatures (895 and 904.5 K) the value of  $n$  increases, possibly indicating that the nucleation rate is beginning to make a significant contribution to the overall rate of transformation.

As has been observed for other metallic glasses [23], the activation energy for crystallization is higher than the values reported in the limited number of diffusion tests performed on metallic glasses [27,28]. Therefore, it is thought that crystallization is governed by some cooperative atomic mechanism rather than the diffusion of a single atomic species.

#### Mechanical Properties

Although the as-quenched  $\text{Ni}_{60}\text{Nb}_{40}$  metallic glass exhibits both high strength and hardness, it is clear that the thermal treatments may significantly alter the properties of the material. As might be expected, the material shows an increase in hardness after the onset of crystallization as hard intermetallic precipitates are formed within the glassy matrix. However, it is also shown that pronounced changes in the mechanical properties may occur prior to crystallization, as exhibited by the observed changes in hardness, tensile strength and ductility. Such effects of structural relaxation are widely observed in metallic glasses [23] as the as-quenched structure relaxes towards a state of lower free energy upon exposure to high temperature.

The embrittlement of the  $\text{Ni}_{60}\text{Nb}_{40}$  prior to crystallization is somewhat surprising but confirms similar observations of Pratten and Scott [29] in this system. Embrittlement has previously been widely reported in metal-metalloid glasses [30,31]. In such cases it is

suggested that the embrittlement is associated with the rapid diffusion and segregation of the small metalloid atoms, notably phosphorous [30], or with the formation of local structural and compositional fluctuations in regions of about 20 Å which produce local stress concentrations [31]. Pratten and Scott suggested in their study that the embrittlement of  $\text{Ni}_{60}\text{Nb}_{40}$  glass might be due to internal oxidation as their glasses were prepared in air making some oxidation unavoidable. However, in the present study the samples were prepared in an He atmosphere and subsequently annealed in a vacuum so it is unlikely that the presence of oxygen leads to the embrittlement.

There is some evidence in the present study that relaxation occurs in a two step process as has been reported for other glasses [32]. A short isothermal anneal at 771 K leads to a very rapid structural change producing a significant increase in hardness and a large reduction in ductility. Further annealing results in a reduction in hardness while producing little further change in ductility until the onset of crystallization. As suggested elsewhere [32], the initial rapid relaxation may be due to very short range atomic rearrangements while the subsequent relaxation may involve larger cooperative atomic rearrangements; although it is not clear why this process reduces hardness.

#### Alloy Development

Although a number of studies of alloying effects in metal-metalloid glasses have been made, very little data are available for metal-metal systems. A number of efforts have been made to correlate the  $T_g$  to various parameters including the melting temperature and atomic radius [33] of the alloying element and the electron to atom ratio of the new glass.

It is of interest to the present case to use an analysis which Giessen et al. [34] have applied to Cu-Zr alloys. They suggest that the change in the glass transition temperature is related to the melting temperature  $T_m$  (M) and the molar volume  $V_m$  of the element by the relation

$$T_g = T_m (M) V_m^{-2/3}$$

This equation is derived from the Lindemann melting point formula for crystalline materials which relates the melting temperature to the Debye temperature and/or Young's modulus. Good agreement was found with this formula for Cu-Zr glasses. Using the crystallization temperature as an estimate of  $T_g$ , which in most alloys was obscured, plots of  $T_x$  versus  $T_m(M)V_m^{-2/3}$  are shown in Fig. 6 for  $(Ni_{60}Nb_{35})M_5$  and  $(Ni_{55}Nb_{40})M_5$  alloys. For both cases there is general agreement although some exceptions are notable. In the  $(Ni_{55}Nb_{40})M_5$  alloys Cu destabilizes the glass to a lesser extent than expected while Fe is more destabilizing than would be anticipated. The effectiveness of copper as a stabilizing element has been shown in a number of studies and is thought to be related to its B-metal character. In the  $(Ni_{60}Nb_{35})M_5$  glasses there is also good general agreement. Tungsten shows some deviation from its expected result, but the more surprising result is the large deviation of vanadium. This is somewhat surprising as V is a member of the same family of the periodic table as Nb and would be expected to behave in a similar manner.

It is apparent from the above results that both the atomic size and the cohesive strength of an alloying element play a role in determining the effect on glass crystallization temperature. The deviations only serve to emphasize the complexity of the alloying problem and illustrate the difficulty of devising new alloys.

The addition of boron proved to be most effective in increasing the crystallization temperature, with a 5 at.% B addition increasing the crystallization temperature by almost 40 K.

These findings are similar to those reported in Cu-Zr where non-transition metal alloying elements were found to have a stabilizing effect [34]. For these elements it was reported that valence and atomic size were pertinent in determining crystallization temperature. Although the addition of B appears most effective in the present study, only limited amounts of the metalloid (~5%) could be added without obtaining some degree of crystallinity in the glass structure.

### CONCLUSIONS

As yet it has not been possible to produce a glass that will transform to a ductile crystalline phase in Ni-Nb. Ternary additions of Mo, Zr, Ni, Si and Al to the Fe-B system are suggested as glass stabilizing agents.

The  $\text{Ni}_{60}\text{Nb}_{40}$  metallic glass exhibits high strength and hardness in combination with good ductility. The glass crystallizes at  $\sim 900$  K. It is believed that the initial step in crystallization is a growth controlled process with activation energy of 6.50 ev. Exposure of the  $\text{Ni}_{60}\text{Nb}_{40}$  glass to high temperature results in embrittlement even prior to the onset of crystallization.

Additions of Mo, Ta and W increased the crystallization temperature of the basic  $\text{Ni}_{60}\text{Nb}_{40}$  alloy. The most effective alloy addition was B but only 5 at.% could be added without inducing some crystallinity in the as-quenched material.

# REFERENCES

1. H. S. Chen, J. Appl. Phys. 49 (1978), 3289.
2. H. S. Chen and E. Coleman, Appl. Phys. Lett. 28 (1976), 245.
3. A. Kursumovic and M. J. Scott, Appl. Phys. Lett. 37 (1980), 620.
4. H. S. Chen, R. C. Sherwood, H. J. Leamy, and E. M. Gyorgy, IEEE Trans. on Magnetics, MAG-12, (1976), 933.
5. R. Ruhl, B. C. Giessen, M. Cohen, and N. J. Grant, Acta Met. 15 (1967), 1693.
6. R. C. Ruhl, B. C. Giessen, M. Cohen, and N. J. Grant, J. Less-Common Metals 13 (1967), 611.
7. H. Jones and C. Suryanarayana, J. Mat. Sci. 8 (1973), 705.
8. H. A. Davies, Rapidly Quenched Metals III, Vol. 1, A-1 (1978), 1.
9. R. Ray, R. Hasegawa, C.-P. Chou, and L. A. Davis, Scripta Met. 11 (1977), 973.
10. H. H. Liebermann, Rapidly Quenched Metals III, Vol. 1, A-4 (1978) 30.
11. A. Inoue, S. Sakai, H. M. Kimura, and T. Masumoto, Trans. JIM 20 (1979), 255.
12. R. H. Willens and E. Buehler, Trans. Met. Soc. AIME 236 (1966), 171.
13. R. Ray and R. Hasegawa, Sol. State Comm. 27 (1978), 471.
14. H. E. Kissinger, Anal. Chem. 29 (1957), 1702.
15. H. Hascke, M. Nowotny, and F. Benesovsky, Monatsh. Chem. 97 (1966), 1459.
16. Yu. B. Kuzima, V. I. Lakh, Yu. V. Voroshilov, B. I. Stadnyk, and V. Ya. Markov, Metally (1965), 88.
17. H. H. Stadelmaier and C. B. Pollock, Z. Metallkde. 60 (1969), 960.
18. M. Naka and T. Masumoto, Sci. Rep. RITU, A27 (1979), 118.
19. H. H. Stadelmaier, R. E. Burgess, and H. H. Davis, Metall. 20 (1966)
20. B. G. Lewis, H. A. Davies, and K. D. Ward, Rapidly Quenched Metals, Vol. 1, C-15 (1978), 325.
21. C. Suryanarayana, Suppl. Sci. Rep. RITU A (1980), 143.
22. B. C. Giessen, M. Madhava, D. E. Polk, and J. Vander Sande, Mat. Sci. Eng. 23 (1976), 145.

23. M. G. Scott, Rapidly Quenched Metals III, ed. B. Cantor, Vol. 1, The Metals Society, London (1978), p. 198.
24. J. Burke, The Kinetics of Phase Transformations in Metals, London, Pergamon (1965).
25. P. G. Boswell, Scripta Met. 11 (1977), 701.
26. N. Funakoshi, T. Kawamari, and T. Manabe, Jpn. J. Appl. Phys. 16 (1977), 515.
27. H. S. Chen, L. C. Kiwerling, J. M. Poate, and W. L. Brown, Appl. Phys. Lett. 32 (1978), 461.
28. C. Birac and D. Lesueur, Phys. Stat. Sol. 36, (1976), 247.
29. N. A. Pratten and M. G. Scott, Scripta Met. 12 (1978), 137.
30. J. L. Walter, F. Bacon and F. E. Luborsky, Mater. Sci. Eng., 24 (1976), 239.
31. H. S. Chen, Mat. Sci. Eng. 26 (1976), 79.
32. H. S. Chen and E. Coleman, Appl. Phys. Lett. 28 (1976), 245.
33. I. W. Donald and H. A. Davies, Rapidly Quenched Metals III, ed. B. Cantor, Vol. 1, The Metals Society, London (1978), p. 273.
34. B. C. Giessen, J. Hang, L. Kabacoff, D. E. Polk, R. Raman, and R. St. Amand, Rapidly Quenched Metals III, ed. B. Cantor, Vol. 1, The Metals Society, London (1978), p. 249.

#### PERSONNEL

During the past 2 to 3 years, two Ph.D. candidates have been assigned full time to this ARO program. They are Laurie Collins and Charles Ashdown. Mr. Collins will probably complete his research by June 1981. Mr. Ashdown, working with ductile, crystallized glasses, will probably complete his research by February 1982. Both candidates have completed all their Ph.D. requirements except the thesis.

Table 1. Data on Experimental Ni-Nb-X Alloys

<u>Composition</u>	<u>Microstructure</u>	<u>Reference</u>
Ni <sub>85</sub> Nb <sub>15</sub>	fcc solid solution (s.s.)	1
Ni <sub>80</sub> Nb <sub>20</sub>	fcc Ni s.s. + metastable hcp	
Ni <sub>79</sub> Nb <sub>14</sub> Al <sub>7</sub>	fcc Ni s.s. + Ni <sub>3</sub> Al + Ni <sub>3</sub> Nb	2
Ni <sub>76</sub> Nb <sub>16</sub> Al <sub>8</sub> *	fcc Ni s.s. + Ni <sub>3</sub> Al + Ni <sub>3</sub> Nb	
Ni <sub>81</sub> Nb <sub>14</sub> B <sub>5</sub>	fcc Ni s.s. + $\tau$ + Ni <sub>3</sub> Nb	3
Ni <sub>80</sub> Nb <sub>7</sub> B <sub>13</sub>	fcc Ni s.s. + $\tau$	
Ni <sub>78</sub> Nb <sub>10</sub> B <sub>12</sub> *	fcc Ni s.s. + $\tau$ + Ni <sub>3</sub> Nb	
Ni <sub>77</sub> Nb <sub>15</sub> C <sub>8</sub>	fcc Ni s.s. + NbC	4
Ni <sub>80</sub> Nb <sub>15</sub> Si <sub>5</sub>	fcc Ni s.s. + Ni <sub>3</sub> Nb + $\lambda$	5
Ni <sub>73</sub> Nb <sub>11</sub> Si <sub>16</sub>	fcc Ni s.s. + $\tau$ + $\lambda$	
Ni <sub>70</sub> Nb <sub>15</sub> Si <sub>15</sub>	fcc Ni s.s. + $\tau$ + $\lambda$	

\*ternary eutectic

1. R. C. Ruhl, B. C. Giessen, M. Cohen, and N. J. Grant, J. Less Common Metals 13 (1967), 611.
2. D. S. Duvall and M. J. Donachie, JIM 98 (1970), 182.
3. J.-D. Schobel and H. H. Stadelmaier, Metall. 18 (1964), 1285.
4. F. D. Lemkey and E. R. Thomson, Met. Trans. 2 (1971), 1537.
5. E. I. Gladyshevski, O. S. Koshe1, and R. V. Skolozdva, Inorg. Mat. 5 (1969), 1882.



Table 2. Crystallization Temperatures of Ni-Nb-M Alloys

<u>Alloy</u>	<u>Structure</u>	<u>T<sub>x</sub> (K)</u>	<u>T<sub>P1</sub> (K)</u>
Ni <sub>60</sub> Nb <sub>40</sub>	A	929	939
Ni <sub>55</sub> Nb <sub>40</sub> Ti <sub>5</sub>	A	894	915
V <sub>5</sub>	P.C.	—	—
Cr <sub>5</sub>	P.C.	—	—
Mn <sub>5</sub>	A	893.5	917
Fe <sub>5</sub>	A	907	923
Co <sub>5</sub>	A	931	941
Cu <sub>5</sub>	A	906	925
<hr/>			
Ni <sub>60</sub> Nb <sub>35</sub> Ti <sub>5</sub>	A	913	922
Zr <sub>5</sub>	A	916	926
Hf <sub>5</sub>	A	921	931
V <sub>5</sub>	A	895.5	916.5
Ta <sub>5</sub>	A	938.5	948
Cr <sub>5</sub>	P.C.	—	—
Mo <sub>5</sub>	A	939.5	950.5
W <sub>5</sub>	A	940	957
<hr/>			
(Ni <sub>60</sub> Nb <sub>40</sub> ) <sub>97.5</sub> B <sub>2.5</sub>	A	944	957
(Ni <sub>60</sub> Nb <sub>40</sub> ) <sub>95</sub> B <sub>5</sub>	A	965	975
(Ni <sub>60</sub> Nb <sub>40</sub> ) <sub>90</sub> B <sub>10</sub>	P.C.	—	—
<hr/>			

Table 2 (continued)

$(\text{Ni}_{60}\text{Nb}_{40})_{97.5}\text{Si}_{2.5}$	A	904	938
$(\text{Ni}_{60}\text{Nb}_{40})_{95}\text{Si}_5$	P.C.	—	—
$(\text{Ni}_{60}\text{Nb}_{40})_{95}\text{Al}_5$	A	896	918.5
$(\text{Ni}_{60}\text{Nb}_{40})_{90}\text{Al}_{10}$	P.C.	—	—

Index: A - Amorphous

P.C. - Partially Crystalline

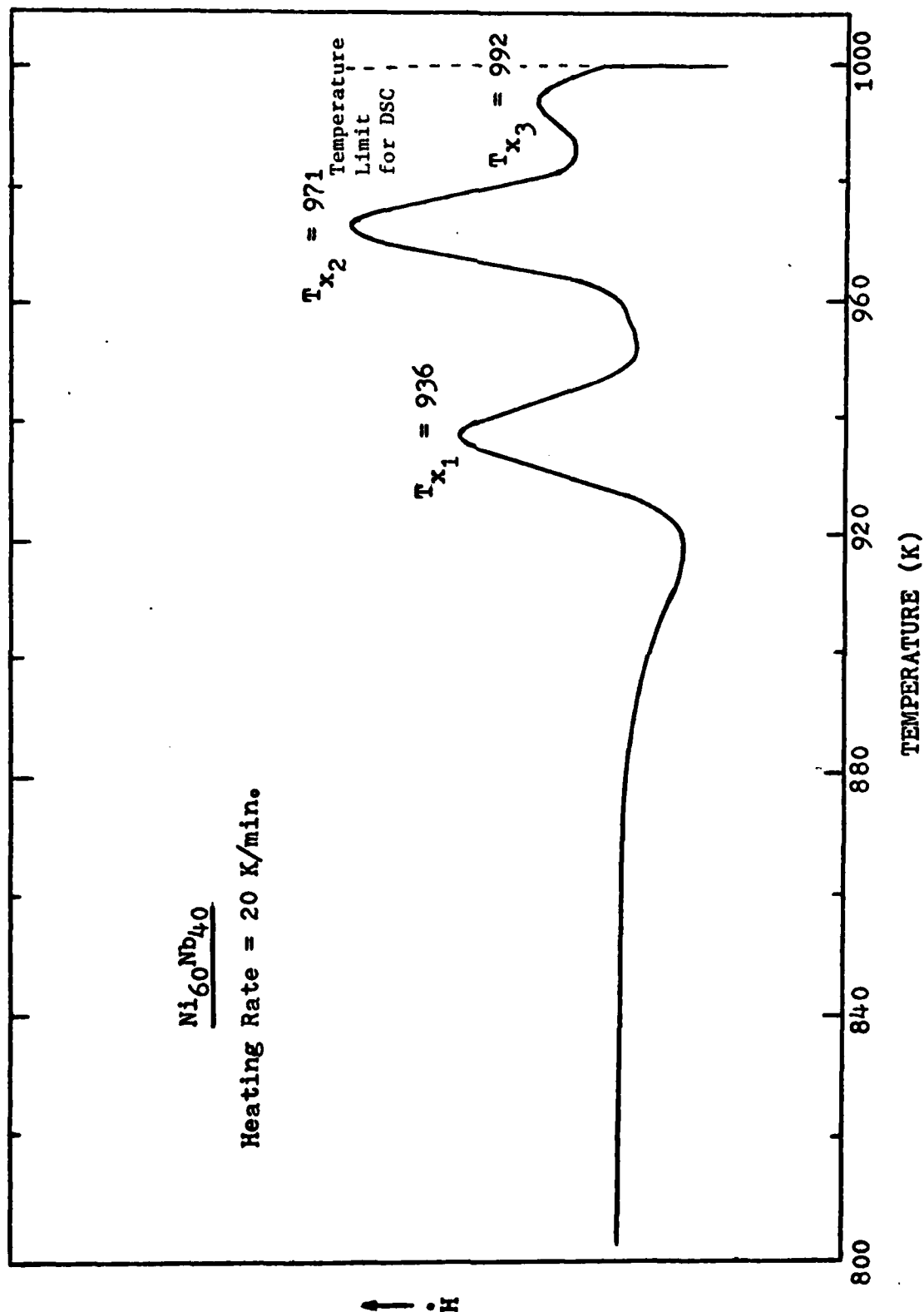


Figure 1. Typical DSC scan showing three exothermic transformations.

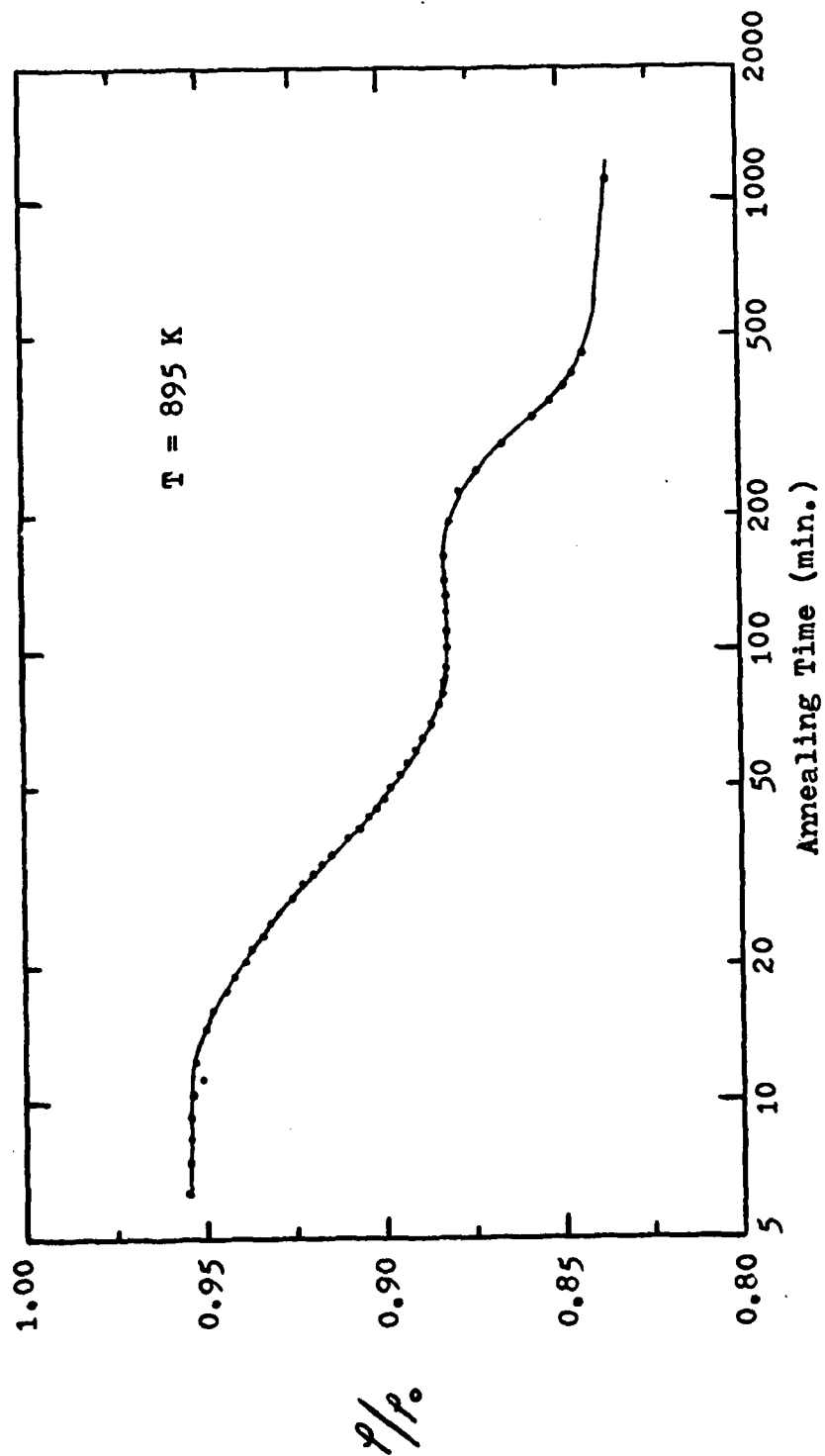


Figure 2. Normalized resistivity measurements obtained during an isothermal anneal of  $\text{Ni}_{60}\text{Nb}_{40}$  at 895 K.

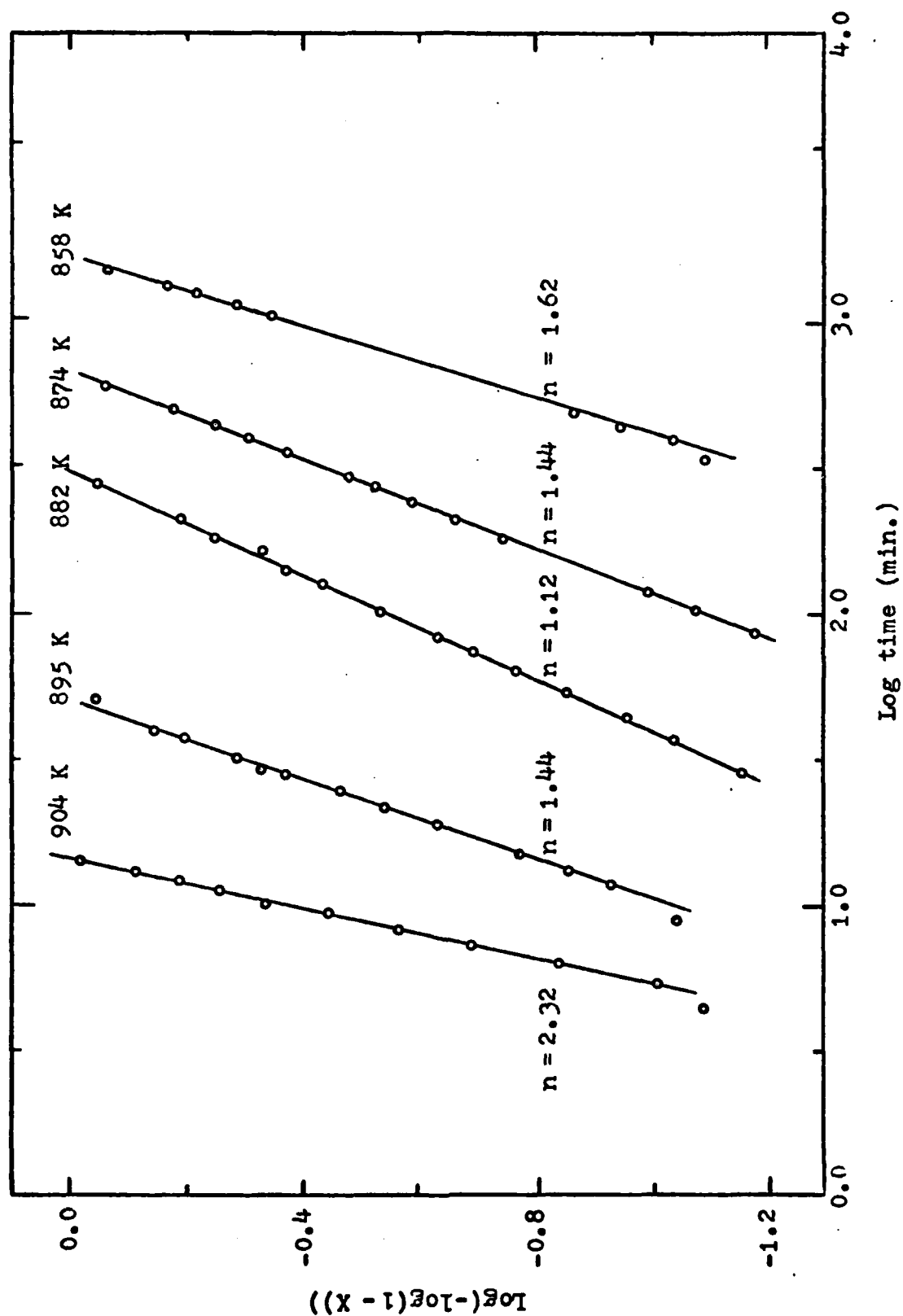


Figure 3. Johnson-Mehl-Avrami plot of resistivity data for the first stage of recrystallization in  $\text{Ni}_{60}\text{Nb}_{40}$ .

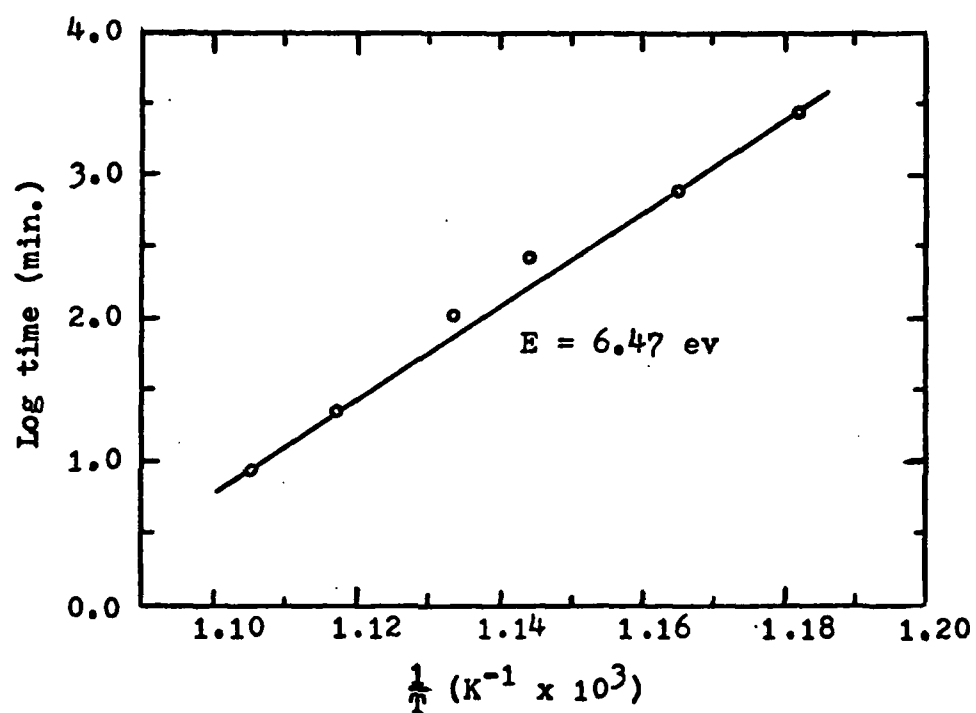


Figure 4. Temperature dependence of the time to achieve 50% completion of the first stage of crystallization in  $\text{Ni}_{60}\text{Nb}_{40}$ .

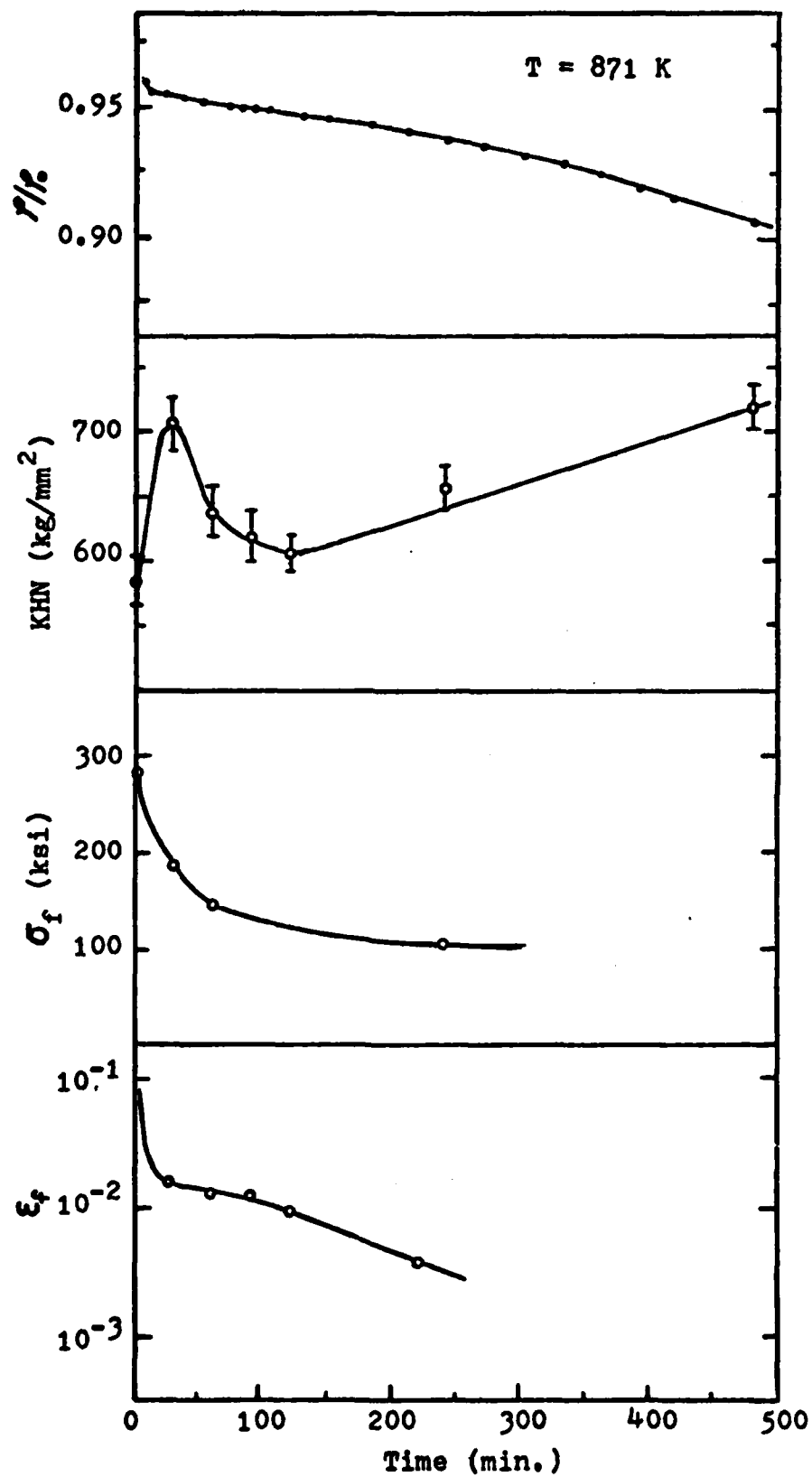


Figure 5. Effect of annealing at 871 K on the room temperature properties of  $\text{Ni}_{60}\text{Nb}_{40}$  glass.

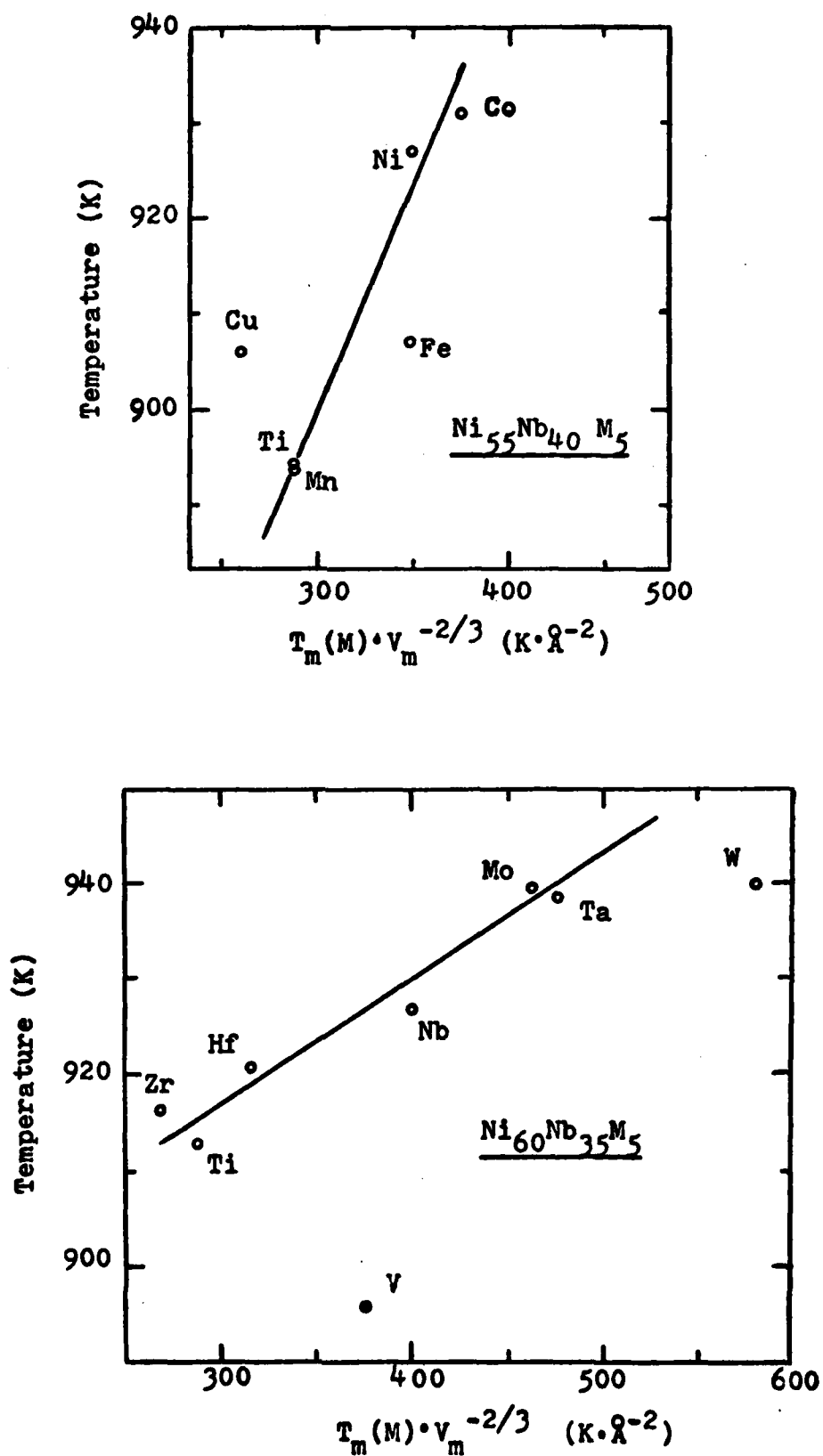


Figure 6. Relation of crystallization temperature to melting temperature and atomic volume of alloying elements in Ni-Nb glasses.